

M²IST: Multi-Modal Interactive Side-Tuning for Efficient Referring Expression Comprehension

Xuyang Liu, Ting Liu, Siteng Huang, Yi Xin, Yue Hu, Long Qin, Donglin Wang, *Member, IEEE*
and Honggang Chen, *Member, IEEE*

Abstract—Referring expression comprehension (REC) is a vision-language task to locate a target object in an image based on a language expression. Fully fine-tuning general-purpose pre-trained vision-language foundation models for REC yields impressive performance but becomes increasingly costly. Parameter-efficient transfer learning (PETL) methods have shown strong performance with fewer tunable parameters. However, directly applying PETL to REC faces two challenges: (1) insufficient multi-modal interaction between pre-trained vision-language foundation models, and (2) high GPU memory usage due to gradients passing through the heavy vision-language foundation models. To this end, we present M²IST: Multi-Modal Interactive Side-Tuning with M³ISAs: Mixture of Multi-Modal Interactive Side-Adapters. During fine-tuning, we keep the pre-trained uni-modal encoders fixed, updating M³ISAs on side networks to progressively connect them, enabling more comprehensive vision-language alignment and efficient tuning for REC. Empirical results reveal that M²IST achieves an optimal balance between performance and efficiency compared to most full fine-tuning and other PETL methods. With M²IST, standard transformer-based REC methods present competitive or even superior performance compared to full fine-tuning, while utilizing only 2.11% of the tunable parameters, 39.61% of the GPU memory, and 63.46% of the fine-tuning time required for full fine-tuning.

Index Terms—Vision-language foundation models, parameter-efficient transfer learning, referring expression comprehension.

I. INTRODUCTION

REFERRING expression comprehension (REC) is one of the most challenging vision-language tasks, aiming to

Xuyang Liu and Ting Liu contributed equally to this work.

This work was supported in part by the National Natural Science Foundation of China (Grant Nos. 62001316, 62306329 and 62103425), in part by Sichuan Science and Technology Program under Grant 2024YFHZ0212, in part by the Open Foundation of Yunnan Key Laboratory of Software Engineering under Grant 2023SE206, and in part by the Fundamental Research Funds for the Central Universities under Grant SCU2023D062 and under Grant 2022CDSN-15-SCU. (*Corresponding author: Honggang Chen.*)

Xuyang Liu is with the College of Electronics and Information Engineering, Sichuan University, Chengdu 610065, China (email: liuxuyang@stu.scu.edu.cn).

Ting Liu, Yue Hu, and Long Qin are with the College of Systems Engineering, National University of Defense Technology, Changsha 410072, China. (email: liuting20@nudt.edu.cn, huyue11@nudt.edu.cn, qinlong@nudt.edu.cn).

Siteng Huang and Donglin Wang are with the School of Engineering, Westlake University, Hangzhou 310030, China (email: siteng.huang@gmail.com, wangdonglin@westlake.edu.cn).

Yi Xin is with the State Key Laboratory for Novel Software Technology, Nanjing University, Nanjing 210000, China (email: xinyi@smail.nju.edu.cn).

Honggang Chen is with the College of Electronics and Information Engineering, Sichuan University, Chengdu 610065, China, and also with the Yunnan Key Laboratory of Software Engineering, Yunnan University, Kunming 650600, China (e-mail: honggang_chen@scu.edu.cn).

locate a specific object in an image based on a given referring expression [1]–[6]. Recent studies [3], [7]–[9] have demonstrated impressive performance by fine-tuning general-purpose vision-language foundation models for this task. However, fully fine-tuning these pre-trained models is computationally expensive when adapting to a new dataset (see Figure 1 (a)). Additionally, fine-tuning on limited REC data may lead to catastrophic forgetting and overfitting, as recently evaluated in other vision-language tasks [10], [11].

Recently, parameter-efficient transfer learning (PETL) methods [12]–[15] have been proposed to address similar issues by updating only a small set of parameters to efficiently adapt pre-trained models to downstream tasks. Adapter-tuning [12], a prominent PETL method, has demonstrated significant success across various vision-language foundation models as well as downstream tasks [11], [16], [17]. It typically inserts a tunable lightweight bottleneck-shaped module sequentially into each frozen backbone layer. Most *transformer-based* REC models [3], [7], [18], [19] use pre-trained Vision Encoder and Language Encoder to separately extract image and text features, which are then integrated to form multi-modality features for reasoning. A straightforward approach to apply adapter-tuning for REC is to insert the adapters into the transformer encoder layers to enhance fine-tuning efficiency (see Figure 1 (b)). However, this introduces *two significant challenges*: (1) Updating inserted adapters still requires backpropagation of gradients through the large pre-trained vision and language models, placing a heavy burden on GPU memory during fine-tuning (see Figure 1 (b)). (2) Vision-language foundation models are pre-trained separately, each with its own structure and training data [20], [21]. Directly inserting vanilla adapters into them may lack cross-modality interaction in the shallow layers of the entire modal, resulting in sub-optimal vision-language alignment. This is particularly problematic for predicting referred objects in cases with complex semantic information, such as human actions and spatial relations (see Figure 4 "Without Interaction").

To address these challenges, we propose a novel **Multi-Modal Interactive Side-Tuning (M²IST)** method that effectively strengthens vision-language alignment and enables parameter- and memory-efficient transfer to REC within the unified *interactive side networks* (see Figure 1 (c)). Specifically, we introduce **Mixture of Multi-Modal Interactive Side-Adapters (M³ISAs)**, which incorporate Vision Expert Adapters (VEA), Language Expert Adapters (LEA), and Interaction Expert Adapters (IEA) into the *side networks* in parallel with the heavy encoders. VEA and LEA transfer pre-trained single-

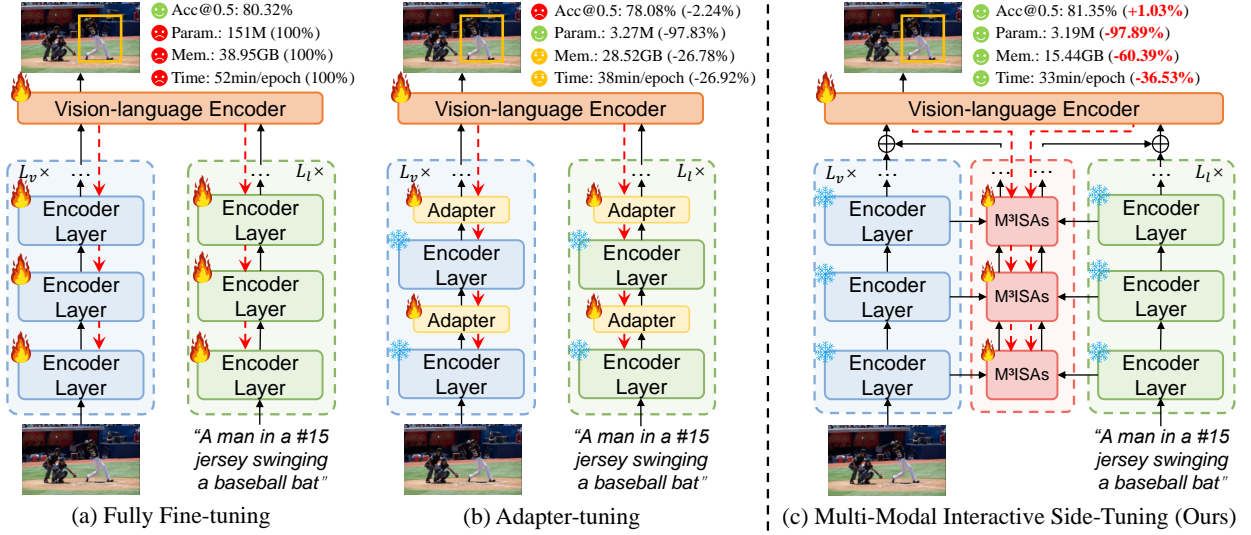


Fig. 1. Comparison of (a) fully fine-tuning, (b) Adapter-tuning, and (c) our M²IST for REC. By only using 2.11% of the tunable parameters, 39.61% of the GPU memory, and 63.46% of the fine-tuning time, M²IST achieves comparable or even superior performance compared to fully fine-tuning.

modality knowledge to the REC domain. IEA utilizes a linear layer for weight-sharing between image and text features, enabling progressive interaction between the referring sentence and input image. Such interaction aggregates *channel-level* vision-language alignment at shallow layers of the model, facilitating deep *token-level* vision-language alignment in deeper layers for improved performance. This elegant design achieves parameter-, memory-, and time-efficient *intra-* and *inter-*modality representation transfer for REC.

We conduct extensive experiments on RefCOCO [22], RefCOCO+ [22], and RefCOCOg [23], [24] to demonstrate the effectiveness and efficiency of M²IST for REC. Experimental results show that M²IST achieves the optimal performance-parameter-memory trade-off compared to most full fine-tuning methods and other PETL methods. By applying our M²IST method, a standard transformer-based REC model can require only **2.11%** of the tunable parameters, **39.61%** of the GPU memory and **63.46%** of the fine-tuning time compared to full fine-tuning, while still achieving competitive performance (see Figure 1). With the sufficient vision-language interaction strengthened by our M³ISAs, our method can accurately locate the referred objects for various complex cases (see Figure 4).

To summarize, our main **contributions** are three-fold:

- 1) We propose M²IST, a novel Multi-Modal Interactive Side-Tuning method for referring expression comprehension (REC), which effectively addresses the challenges of insufficient multi-modal interaction and high GPU memory consumption in applying parameter-efficient transfer learning (PETL) to REC.
- 2) We design Mixture of Multi-Modal Interactive Side Adapters (M³ISAs), seamlessly integrating pre-trained vision and language encoders, enabling parameter-, memory-, and time-efficient tuning within a unified interactive side network for REC.
- 3) We conduct empirical studies on the application of PETL methods in REC, highlighting their limitations in practical scenarios. Extensive experiments on three widely-

used benchmarks validate the effectiveness of M²IST, achieving the optimal trade-off between performance and efficiency compared to full fine-tuning and other PETL methods, with significantly reduced GPU memory usage and fine-tuning time.

II. RELATED WORK

A. Referring Expression Comprehension

Referring expression comprehension (REC) [1]–[4], [7], [9], [25], [26] aims to locate the specific objects in images based on textual descriptions.

Early REC methods [1], [27], [28] follow a *two-stage* pipeline that first uses a pre-trained object detector (e.g., Faster R-CNN [29]) to generate a set of sparse object proposals, which are then ranked by their similarity to the given textual description. MAttNet [1] uses Faster R-CNN to generate object proposals, then scores them based on the referring expression to find the most relevant object. RvG-Tree [30] builds a relational visual graph to capture object interactions and ranks proposals according to their relevance to the expression, improving grounding accuracy. However, these *two-stage* REC methods heavily rely on the quality of the object proposals and cannot directly predict the referred object region. *One-stage* anchor-based methods [2], [31]–[33] have been developed to eliminate the proposal generation step, directly predicting object bounding boxes from predefined anchors [34]. FAOA [2] utilizes the YOLOv3 detector [34], integrating it with an encoded language vector to ground the referred regions. MRLN [4] introduces three modules: feature-feature relational learning, feature-task relational learning, and task-task relational learning, to enhance the collaborative learning of REC, effectively reducing prediction inconsistency in multi-task learning. Recently, *transformer-based* methods [3], [7], [9], [26], [35] have demonstrated superior performance by implicitly modeling cross-modality relationships within a unified architecture. The pioneering work TransVG [3] applies a stack of transformer encoders to perform feature extraction and

multi-modal fusion for REC. VGTR [35] employs a transformer encoder-decoder architecture to jointly reason over visual and textual inputs, grounding the referred object without relying on pre-trained detectors or word embeddings. Dynamic M-DETR [9] uses a dynamic multi-modal transformer decoder to adaptively sample visual features and perform text-guided decoding for REC.

As REC models continue to scale up, their performance has improved. However, this performance gain comes at the cost of increased computational cost, which demands larger GPU memory for more parameter fitting (see Figure 1 (a)).

B. Parameter-efficient Transfer Learning

Parameter-efficient transfer learning (PETL) [12]–[15] has emerged as a promising alternative to fully fine-tuning pre-trained models for downstream tasks. By updating only a minimal subset of parameters, PETL methods balance performance and computational efficiency.

Recent PETL methods can be classified into two categories. The first category is updating additional parameters in modules inserted into the model [12], [15], [36] or appended to the input data [14], [37], [38]. Adapter [12] incorporates a bottleneck module into each Transformer layer, positioned after both the Multi-Head Attention (MHA) and the Feed-Forward Networks (FFN). AdaptFormer [15] embeds the adapter module parallel to the FFN in each encoder of a Vision Transformer. VPT [14] appends learnable visual vectors to the input sequences (VPT-Shallow) or to the input of each transformer encoder layer (VPT-Deep). The second category involves decomposing weight matrices into two low-rank matrices and updating only the small factorization matrices [13], [39]. As a pioneering work, LoRA [13] integrates a tunable pair of low-rank decomposed weight matrices into each encoder layer of the pre-trained networks. FacT [39] incorporates tunable factorized weight matrices into each layer of the pre-trained networks. There is also growing interest in adapter-based PETL methods for vision-language tasks, including text-image retrieval [11] and text-video retrieval [40], [41]. Most of these methods aim to achieve effective cross-modality interaction while maintaining parameter efficiency.

However, existing PETL methods still face substantial GPU memory consumption during the fine-tuning stage, as gradients must propagate through the heavy pre-trained encoders for REC (see Figure 1 (b)).

C. Memory-efficient Transfer Learning

Memory-efficient transfer learning (METL) [42]–[44] aims to reduce memory costs on GPUs during fine-tuning. Existing METL methods typically employ a *side network* for single-modality knowledge transfer, focusing on either NLP [43] or CV [44] downstream tasks. Side-Tuning [42] utilized an additional side network that adds its representation to the backbone network in the last layer. LST [43] adopted a separate and lightweight side network with the same architecture as the pre-trained model but reduced each layer dimension by a pre-defined reduction factor. DTL [44] disentangled the weights update from the pre-trained backbone network by proposing

a lightweight side network, which achieved high accuracy in classification with low GPU memory usage.

In this work, inspired by the existing efforts, our M²IST bridges the pre-trained Vision Encoder and Language Encoder through the unified *side interactive networks*, enabling a parameter-, memory-, and time-efficient transfer to the REC task (see Figure 1 (c)).

III. METHODOLOGY

In this section, we present our M²IST in detail. First, we briefly overview the base architecture for referring expression comprehension in Section III-A. Then, we elaborate on the designs of our efficient tuning method M²IST and its core component M³ISA in Section III-B. Finally, we provide an in-depth analysis of some advantages of M²IST in Section III-C.

A. Base Architecture

We apply a standard *transformer-based* REC model as our base architecture, shown in Figure 1 (a), which comprises: (1) a Vision Encoder, (2) a Language Encoder, and (3) a Vision-language Encoder.

a) *Vision Encoder*: We adopt a DETR-based [20] encoder as our Vision Encoder, which comprises a ResNet [45] and a stack of transformer encoder layers to encode the image into high-quality vision embeddings. Specifically, given an input image $z_0 \in \mathbb{R}^{H_0 \times W_0 \times 3}$, the ResNet is utilized to generate a 2D feature map $z \in \mathbb{R}^{H \times W \times C}$, where H_0 and W_0 denote the height and width of the input image, $H = \frac{H_0}{32}$, $W = \frac{W_0}{32}$, and $C = 2048$ represents the channel dimension. Then, a 1×1 convolutional layer reduces the C to $C_v = 256$, producing $z' \in \mathbb{R}^{H \times W \times C_v}$. We flatten the feature map z' into a sequence of 1D vectors (i.e., vision tokens) $z_v \in \mathbb{R}^{N_v \times C_v}$, where $N_v = H \times W$ indicates the number of tokens. Sequentially, these vision tokens added with positional encodings are fed into a stack of 6 transformer encoder layers, which then output the enhanced vision embeddings $f_v \in \mathbb{R}^{N_v \times C_v}$ incorporating global context of the image.

b) *Language Encoder*: We employ an off-the-shelf language model BERT [21], comprising a stack of transformer encoder layers, as our Language Encoder. Specifically, given the input text, each word ID is converted into a one-hot vector, which is then tokenized into a sequence of language tokens. These language tokens, concatenated with a [CLS] token at the beginning and a [SEP] token at the end, are input to 12 transformer encoder layers to sequentially model contextual relationships. Similar to the Vision Encoder, Language Encoder finally outputs the enhanced language embeddings $f_l \in \mathbb{R}^{N_l \times C_l}$, where N_l and $C_l = 768$ represent the number and channel dimension of language tokens, respectively.

c) *Vision-language Encoder*: We use a transformer-based encoder [46] as our Vision-language Encoder (V-L Encoder) to thoroughly fuse the multi-modality embeddings and predict the bounding box of the referred object. Specifically, the enhanced vision embeddings $f_v \in \mathbb{R}^{N_v \times C_v}$ and language embeddings $f_l \in \mathbb{R}^{N_l \times C_l}$ are first projected into the joint embeddings $f'_v \in \mathbb{R}^{N_v \times C_p}$ and $f'_l \in \mathbb{R}^{N_l \times C_p}$, sharing the same channel dimension $C_p = 256$. The joint embeddings, along with a

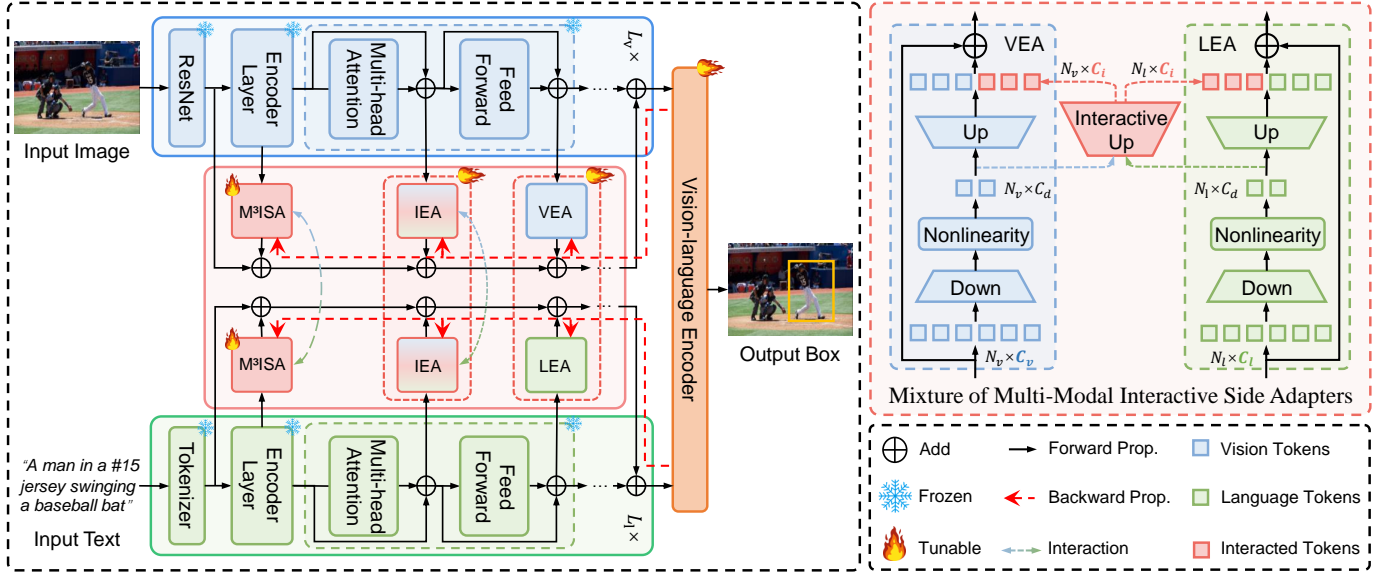


Fig. 2. **Overall architecture of M²IST.** M²IST freezes the pre-trained Vision Encoder (blue branch) and Language Encoder (green branch), while updating M³ISAs on *side networks* (pink branch). M³ISAs comprise IEA for bridging the pre-trained dual encoders to enable cross-modality interactions, and VEA/LEA for transferring pre-trained single-modality representations to adapt to the REC domain. By avoiding backpropagation through the heavy encoders (red dashed arrow), M²IST enables **parameter-, memory-, and time-efficient** tuning for the task of referring expression comprehension.

learnable [REG] token, are then fed into a stack of 6 transformer encoder layers to fuse the cross-modality embeddings and output the [REG] token. Finally, a prediction head, implemented as a Multi-layer Perceptron with two 256-dim hidden layers and a linear output layer, receives the [REG] token and regresses it to the 4-dim box coordinates for the referred object.

B. Multi-Modal Interactive Side-Tuning: M²IST

Given that the pre-trained vision and language encoders contain rich knowledge and comprise about 95% of the model’s parameters. We first explore two approaches to reduce training overhead:

- 1) **Fully freezing the pre-trained encoders.** We choose to directly keep the pre-trained parameters fixed and only fine-tune the V-L Encoder. While it effectively saves a significant amount of GPU memory, it also results in significantly inferior performance (see Table V (a)).
- 2) **Updating a few additional parameters.** We explore various mainstream PETL methods, such as Adapter [12] and LoRA [13]. Though most of them achieve relatively satisfactory performance as well as save tunable parameters, updating the additional parameters still necessitates substantial GPU memory rather than effectively mitigating the computational load (see Table I).

To address the above issues, we propose Multi-Modal Interactive Side-Tuning (M²IST) that keeps the pre-trained encoders frozen and updates the proposed Mixture of Multi-Modal Interactive Side Adapters (M³ISA) on *side networks* to facilitate parameter- and memory-efficient fine-tuning for REC, as shown in Figure 2. Note that we do not show the LayerNorm for simplicity.

a) **M³ISA Architecture:** The core component of our M²IST is M³ISA (see Figure 2 (right)), which consists of two distinct adapters, i.e., **intra-** and **inter-**modality adapters to

effectively and efficiently bridge the pre-trained Vision Encoder and Language Encoder.

The intra-modality adapters include **Vision Expert Adapter** (VEA) and **Language Expert Adapter** (LEA), shown as separate blue branch and green branch in Figure 2 (right). They adhere to a fundamental design [12] for transferring pre-trained single-modality representations to more domain-specific ones. Specifically, both of them consist of a down-projection layer \mathbf{W}_{down} , ReLU non-linear activation, and an up-projection layer \mathbf{W}_{up} in sequence. Taking the VEA as a formulaic example, given the vision tokens $\mathbf{x}_v \in \mathbb{R}^{N_v \times C_v}$, the function of VEA can be formally expressed as:

$$\text{VEA}(\mathbf{x}_v) = \mathbf{x}_v + s \cdot \text{ReLU}(\mathbf{x}_v \mathbf{W}_{\text{down}}) \mathbf{W}_{\text{up}}, \quad (1)$$

where $\mathbf{W}_{\text{down}} \in \mathbb{R}^{C_v \times C_d}$, $\mathbf{W}_{\text{up}} \in \mathbb{R}^{C_d \times C_v}$ and s is the scaling factor of the adapter.

In the base architecture, the Vision Encoder and Language Encoder are responsible for extracting single-modality features, while only the V-L encoder is tasked with cross-modality fusion through **token-level** vision-language alignment. However, such the late fusion has been proved insufficient when the referring sentence contains complex semantic information, such as spatial relationships [47]. Therefore, we introduce an inter-modality adapter, named the Interaction Expert Adapter (IEA). Specifically, each IEA shares a set of tokens within the same channel dimensions C_i (i.e., Interacted Tokens in Figure 2 (right)) between the Vision Encoder and Language Encoder, thereby achieving **channel-level** vision-language alignment during the multi-modal feature extraction stage. As depicted by the entire pink section in Figure 2 (right), IEA include a unique down-projection layer for vision $\mathbf{W}_{\text{down}} \in \mathbb{R}^{C_v \times C_d}$ and language $\mathbf{W}_{\text{down}} \in \mathbb{R}^{C_l \times C_d}$, ReLU activation, an interactive up-projection layer $\mathbf{W}_{\text{up}} \in \mathbb{R}^{C_d \times C_i}$, and a unique up-projection layer for vision $\mathbf{W}_{\text{up}} \in \mathbb{R}^{C_d \times (C_v - C_i)}$ and

language $\mathbf{W}_{\text{up}} \in \mathbb{R}^{C_d \times (C_l - C_i)}$, where C_v , C_l , and C_i represent the vision, language, and interaction channels, respectively. Given the vision tokens $\mathbf{x}_v \in \mathbb{R}^{N_v \times C_v}$ and language tokens $\mathbf{x}_l \in \mathbb{R}^{N_l \times C_l}$, the corresponding down-projection layers first down-sample them to the bottleneck features $\mathbf{z}_v \in \mathbb{R}^{N_v \times C_d}$ and $\mathbf{z}_l \in \mathbb{R}^{N_l \times C_d}$. Then, the corresponding up-projection layers and interactive up-projection layer up-sample these bottleneck features and concatenate them within the same modality to obtain the cross-modality features $\mathbf{f}_v \in \mathbb{R}^{N_v \times C_v}$ and $\mathbf{f}_l \in \mathbb{R}^{N_l \times C_l}$ as:

$$\mathbf{f}_v = \text{Concat}[\mathbf{z}_v \mathbf{W}_{\text{up}}, \mathbf{z}_v \mathbf{W}_{\text{up}}], \quad (2)$$

$$\mathbf{f}_l = \text{Concat}[\mathbf{z}_l \mathbf{W}_{\text{up}}, \mathbf{z}_l \mathbf{W}_{\text{up}}]. \quad (3)$$

The outputs of the IEA can be written as:

$$\text{IEA}(x_v) = x_v + s \cdot \mathbf{f}_v, \quad (4)$$

$$\text{IEA}(x_l) = x_l + s \cdot \mathbf{f}_l, \quad (5)$$

where x_v and x_l indicate input as vision tokens and language tokens, respectively.

Our IEA enables lightweight adaptation of cross-modality representations without increasing the explicit computational burden of vision-language feature extraction, thereby efficiently bridging the pre-trained vision and language encoders. Our experimental results in Table IX further demonstrate that deeper *channel-level* vision-language alignment yields better performance for REC. Moreover, such alignment will further improve the *token-level* vision-language alignment in V-L Encoder, leading to better region-sentence understanding in challenging REC scenarios, as analyzed in Section IV-E.

b) M³ISA Implementation: As depicted in Figure 2 (left), we incorporate a stack of M³ISAs into two *side networks* that operate *in parallel* with the pre-trained dual encoders. Specifically, in one encoder layer (both for vision and language), the IEA first receives processed vision/language tokens from the Multi-head Attention (MHA) layers as input and produces adapted, interacted tokens for the vision/language side network. Subsequently, the VEA/LEA take the processed vision/language tokens from the Feed Forward Networks (FFN) as input and generate adapted single-modality tokens for the corresponding side networks. The outputs of the IEA and VEA/LEA are added within the vision/language side networks, along with the original vision/language tokens through skip-connections. After passing through the side networks, the outputs of the vision/language side networks are added to the outputs of the vision/language encoders. During fine-tuning, we keep the pre-trained encoders fixed and update the M³ISAs in the *side networks*, allowing the pre-trained encoders to act as *standalone feature extractors*.

c) Training Objectiveness: Following most *transformer-based* REC methods [3], [9], [26], the training loss function is a combination of the widely used smooth L1 loss and GIoU loss. Specifically, the prediction is denoted as $\mathbf{b} = (x, y, w, h)$, and the normalized ground-truth box as $\hat{\mathbf{b}} = (\hat{x}, \hat{y}, \hat{w}, \hat{h})$. The training objective is:

$$\mathcal{L} = \mathcal{L}_{\text{smooth-l1}}(\mathbf{b}, \hat{\mathbf{b}}) + \lambda \cdot \mathcal{L}_{\text{giou}}(\mathbf{b}, \hat{\mathbf{b}}), \quad (6)$$

where $\mathcal{L}_{\text{smooth-l1}}(\cdot)$ and $\mathcal{L}_{\text{giou}}(\cdot)$ are the smooth L1 loss and GIoU loss. λ is the weight coefficient of GIoU loss to balance these two losses.

C. Discussion: Advantages of M²IST

The proposed M²IST offers several advantages over fully fine-tuning and other PETL methods for REC, which we can summarize as *three efficiency factors*:

- 1) **Parameter Efficiency.** Fully fine-tuning pre-trained vision-language foundation models is computationally expensive due to their large size and complexity [5], [48]. Furthermore, it often leads to forgetting valuable pre-trained knowledge and increases the risk of overfitting, as the encoders are fine-tuned on limited data. M²IST mitigates these issues by freezing the pre-trained encoders and updating only the lightweight M³ISAs, achieving effective intra- and inter-modality representation adaptation and enhanced performance.
- 2) **Memory Efficiency.** Both full fine-tuning and other PETL methods require backpropagation through large pre-trained vision-language foundation models, leading to high GPU memory usage [43], [44]. M²IST reduces this by separating tunable parameters from the pre-trained encoders and placing them in parallel *side interactive networks*. Since gradients backpropagate through the lightweight M³ISAs instead of the heavy encoders, where we only need to store the parameters of our side networks, this leads to reduced GPU memory requirements. Additionally, M²IST maintains the baseline model's architecture, simplifying its implementation compared to other PETL methods.
- 3) **Time Efficiency.** Most PETL methods are able to enhance the speed of fine-tuning compared to full fine-tuning, primarily due to the reduced number of updated parameters. Compared to other PETL methods, our M²IST may offer greater both fine-tuning and inference time efficiency. As for the fine-tuning stage, M²IST introduces tunable parameters in parallel with the pre-trained encoders, allowing gradient computation to occur in the lightweight M³ISAs instead of the computationally intensive encoders. As for the inference stage, compared to most PETL methods that introduce new parameters into the pre-trained networks, compromising inference efficiency, our M²IST can process the additional parameters and the pre-trained networks in parallel, making the inference more efficient.

Therefore, our approach offers parameter-, memory-, and time-efficient adaptation for visual-language foundational models, and enhances the REC task with more comprehensive visual-language alignment.

IV. EXPERIMENTS

In this section, we first introduce the datasets and evaluation metrics used to assess the performance and efficiency of our method in Section IV-A. Next, we describe the implementation details in Section IV-B. Section IV-C provides comprehensive

TABLE I

COMPARISON WITH PETL METHODS USING THE SAME BASE ARCHITECTURE. "PARAM." INDICATES THE NUMBER OF TUNABLE PARAMETERS IN THE PRE-TRAINED ENCODERS. "MEM." DENOTES THE PEAK GPU MEMORY FOOTPRINT WITH BATCH SIZE 64 DURING FINE-TUNING. WE HIGHLIGHT THE BEST AND THE SECOND RESULTS.

Methods	Params.↓ (M)	Mem.↓ (GB)	RefCOCO			RefCOCO+			RefCOCOg		
			val	testA	testB	val	testA	testB	val-g	val-u	test-u
Fully fine-tuning	151 (100%)	38.95 (100%)	80.32	82.67	75.24	63.50	68.15	55.63	66.56	67.66	67.44
Adapter [12]	3.27 (2.17%)	28.52 (73.22%)	<u>78.02</u>	<u>79.89</u>	<u>75.23</u>	<u>61.35</u>	66.34	<u>54.21</u>	63.18	65.26	66.65
LoRA [13]	2.37 (1.57%)	20.37 (52.30%)	77.57	78.22	73.37	61.24	<u>66.53</u>	53.95	<u>64.27</u>	<u>67.36</u>	66.43
AdaptFormer [15]	2.38 (1.57%)	20.37 (52.30%)	76.32	77.16	73.94	60.96	65.19	53.88	61.81	65.44	64.37
CM Adapter [40]	3.27 (2.17%)	27.19 (69.81%)	77.37	78.81	74.07	61.34	66.10	53.31	63.93	65.75	64.72
MRS-Adapter [11]	1.58 (1.05%)	20.07 (51.53%)	77.14	77.80	74.80	61.13	66.38	53.13	63.07	66.46	<u>65.16</u>
M²IST (Ours)	3.19 (2.11%)	15.44 (39.64%)	81.35	82.29	77.98	63.15	67.11	55.52	67.50	67.67	67.41

comparisons of performance and fine-tuning efficiency, followed by an extensive ablative study and analysis of design choices in Section IV-D. Finally, we present multiple qualitative results to analyze model behavior in Section IV-E.

A. Datasets and Evaluation Metrics

a) *Datasets*: To verify the effectiveness and efficiency of our method, we conduct experiments on the following REC benchmarks as follows: (1) *RefCOCO* [22] consists of 19,994 images with 142,210 referring expressions for 50,000 objects. The RefCOCO dataset is officially split into train, validation, testA, and testB sets containing 120,624, 10,834, 5,657, and 5,095 expressions, respectively. (2) *RefCOCO+* [22] includes 19,922 images with 141,564 referring expressions for 49,856 objects. Compared to RefCOCO, the referring expressions in RefCOCO+ focus more on attributes of the referred objects, such as color and shape, without including any positional words. (3) *RefCOCOg* [23], [24] contains 25,799 images with 95,010 referring expressions for 49,822 objects. Compared to RefCOCO and RefCOCO+, the referring expressions in RefCOCOg are typically longer, averaging almost twice the length of those in the other two datasets. RefCOCOg has two commonly used split strategies: the *google* split [23] (-g) and the *umd* split [24] (-u).

b) *Evaluation Metrics*: Following previous work [3], [25], [26], we conduct experiments on both RefCOCOg-g (val-g) and RefCOCOg-u (val-u and test-u). We use Precision@0.5 as the evaluation metric. In addition to accuracy, we also report the number of tunable parameters in the pre-trained encoders and the training memory consumption in Gigabytes (GB) to compare the fine-tuning efficiency with other PETL methods.

B. Implementation Details

a) *Model Weights*: The Vision Encoder is initialized with the backbone (i.e., ResNet-50 [45]) and encoder weights from DETR [20], which is pre-trained on the entire MS-COCO dataset [49]. Specifically, during the pre-training of the Vision Encoder, images from the validation and test sets of RefCOCO+/g that overlap with MS-COCO [49] are excluded. The Language Encoder is initialized with BERT-base [21], pre-trained on the BookCorpus [50] and English Wikipedia [21]. The Vision-Language (V-L) Encoder is initialized using Xavier initialization. The proposed M³ISAs are initialized with Kaiming normal initialization.

b) *Hyper-parameters Settings*: M³ISAs are inserted into the transformer encoder layers at the same indices as those in the Vision Encoder and Language Encoder, and relevant ablation study is conducted in Table VIII. Unless otherwise specified, the bottleneck dimensions of the Visual Expert Adapter (VEA) and Language Expert Adapter (LEA) C_d are set to 128 by default, while the interaction dimension C_i of the Interaction Expert Adapter (IEA) is 256 by default. The scaling factor s for all adapters is set to 0.1.

c) *Training Details*: For RefCOCO [22] and RefCOCOg [23], [24] datasets, the entire network is trained for 90 epochs using the AdamW optimizer, with a learning rate of 10^{-4} for the V-L Encoder and 10^{-5} for the M³ISAs. The weight decay is 10^{-4} , and the learning rate is reduced by a factor of 10 after 60 epochs. While for RefCOCO+ [22], the network is trained for 180 epochs with the same learning rates and weight decay, but the learning rate is decreased by a factor of 10 after 120 epochs. All experiments are conducted on one A800 GPU.

C. Main Results

In this sub-section, we compare our M²IST under different settings to evaluate its performance and the *three efficiency factors* discussed in Section III-C.

a) *Comparison with PETL Methods*: We first compare our proposed M²IST method with several existing parameter-efficient transfer learning (PETL) approaches, using the same base architecture and the same bottleneck dimensions for the adapter modules ($C_d = 128$). These PETL methods include vanilla Adapter [12], LoRA [13], AdaptFormer [15], CM Adapter [40], and MRS-Adapter [11].

From Table I, we can see that all PETL methods including M²IST achieve significant parameter efficiency during fine-tuning by reducing the number of tunable parameters compared to full fine-tuning. Despite the parameter efficiency achieved by these PETL methods, they still face two major limitations in practical applications: a) All methods exhibit performance degradation compared to full fine-tuning. b) They require substantial GPU memory during fine-tuning, thus failing to deliver the efficiency that is crucial during implementation.

As for the performance, M²IST stands out as the only PETL method that can achieve performance on par with or even better than full fine-tuning, significantly outperforming other PETL methods across all three benchmarks. This highlights the

TABLE II
COMPARISON WITH FULL FINE-TUNING ON RefCOCO, RefCOCO+, AND RefCOCOg. "RN50" AND "RN101" REPRESENT RESNET-50 [45], RESNET-101 [45]. "PARAMS." IS THE NUMBER AND AVERAGE PERCENTAGE OF TUNED PARAMETERS IN THE ENCODERS.

Methods	Vision Encoder	Language Encoder	Params.↓ (M)	RefCOCO			RefCOCO+			RefCOCOg		
				val	testA	testB	val	testA	testB	val-g	val-u	test-u
Two-stage:												
VC [51]	VGG16	LSTM	17 (100%)	-	73.33	67.44	-	58.40	53.18	62.30	-	-
ParalAttn [52]	VGG16	LSTM	17 (100%)	-	75.31	65.52	-	61.34	50.86	58.03	-	-
MAttNet [1]	RN101	LSTM	47 (100%)	76.65	81.14	69.99	65.33	71.62	56.00	-	66.58	67.27
RvG-Tree [30]	RN101	LSTM	47 (100%)	75.06	78.61	69.85	63.51	67.45	56.66	-	66.95	66.51
One-stage:												
FAOA [2]	DarkNet-53	LSTM	43 (100%)	72.54	74.35	68.50	56.81	60.23	49.60	56.12	61.33	60.26
RCCF [53]	DLA34	LSTM	18 (100%)	-	81.06	71.85	-	70.35	56.32	-	-	65.73
ReSC [32]	DarkNet-53	BERT	152 (100%)	76.59	78.22	73.25	63.23	66.64	55.53	63.12	67.30	67.20
RealGIN [54]	DarkNet-53	GRU	41 (100%)	77.25	78.70	72.10	62.78	67.17	54.21	-	62.75	62.33
TRAR [55]	DarkNet-53	LSTM	43 (100%)	-	79.60	71.30	-	65.10	53.50	-	63.30	62.50
TransVG [3]	RN50+DETR	BERT	151 (100%)	80.32	82.67	75.24	63.50	68.15	55.63	66.56	67.66	67.44
VGTR [35]	RN50	LSTM	52 (100%)	78.70	82.09	73.31	63.57	69.65	55.33	62.88	65.62	65.30
PFOS [7]	DarkNet-53	BERT	152 (100%)	77.37	80.43	72.87	63.74	68.54	55.84	61.46	67.08	66.35
DMRNet [56]	DarkNet-53	BERT	152 (100%)	76.99	79.71	72.67	61.58	66.60	54.00	-	66.03	66.70
MRLN [4]	VGG16	GRU	18 (100%)	<u>81.39</u>	83.65	75.03	66.33	69.75	58.05	-	65.52	65.08
D-MDETR [9]	RN50+DETR	BERT	143 (100%)	80.47	82.63	75.96	<u>65.52</u>	<u>70.41</u>	<u>57.68</u>	<u>66.87</u>	69.20	68.56
Ours:												
M²IST ($C_d = 8$)	RN50+DETR	BERT	1.91 (1.26%)	81.55	<u>83.07</u>	77.31	62.73	66.96	55.93	65.47	66.79	66.30
M²IST ($C_d = 32$)	RN50+DETR	BERT	2.20 (1.46%)	81.03	82.34	<u>77.54</u>	62.48	66.73	55.70	66.22	67.42	<u>67.83</u>
M²IST ($C_d = 128$)	RN50+DETR	BERT	3.19 (2.11%)	81.35	82.29	77.98	63.15	67.11	55.52	67.50	<u>67.67</u>	67.41

effectiveness of M³ISAs in adapting pre-trained knowledge for the REC task. We can observe that all PETL methods exhibit distinct performance degradation compared to full fine-tuning on the RefCOCOg dataset. This is because RefCOCOg is a substantial dataset with sufficient data, reducing the likelihood of overfitting when fully fine-tuning the models. Even so, with the facilitation of cross-modality interaction between the encoders, M³ISAs are able to enhance the modeling of complex spatial relationships, leading to competitive performance with full fine-tuning on the RefCOCOg benchmark.

Regarding fine-tuning efficiency, M²IST requires the least training memory among PETL methods. This results from the fact that gradients backpropagate through the lightweight M³ISAs rather than the heavy encoders, highlighting M²IST's advantage in **memory efficiency**, as mentioned in Section III-C.

b) Comparison with Full Fine-tuning Methods: We further compare our M²IST with traditional full fine-tuned REC methods in Table II.

Table II demonstrates that M²IST achieves competitive performance across three benchmarks compared to most full fine-tuning methods with the fewest (only 1.91%) trainable backbone parameters. Specifically, on the three sets of RefCOCO [22], M²IST outperforms the majority of other fully fine-tuning REC methods. We can observe that MAttNet [1] and MRLN [4] achieve impressive performance in RefCOCO+ [22]. As a *Two-stage* REC method, MAttNet introduces modular attention networks to separately model the subject, location, and relationship, which can more explicitly locate the referred objects by directly computing the similarity scores between the region proposals and the sentences, thus leading to enhanced performance in RefCOCO+. Similarly, the multiple relational learning modules in MRLN are also well-suited

TABLE III
COMPARISONS OF TRAINING AND INFERENCE SPEED. "FULL" REPRESENTS FULLY FINE-TUNING THE BASELINE MODAL. "TRAINING" DENOTES TRAINING ON RefCOCO, WHILE "INFERENCE" DENOTES INFERENCE TIME ON RefCOCO VAL.

Speed	Full	Adapter	M ² IST
Training (min/epoch) ↓	52	38	33
Inference (s) ↓	145	146	145

to capture these structured and compositional representations of the vision-language interactions. This allows MRLN to excel on the RefCOCO and RefCOCO+, where the referring expressions tend to have a more well-defined structure and can be more effectively represented through the learned feature-feature, feature-task, and task-task relationships. However, as the referring expressions become longer and more complex (i.e., RefCOCOg [23], [24]), the limitations of methods that rely heavily on structured representation learning (MAttNet and MRLN) become more apparent. In contrast, transformer-based approaches (e.g., TransVG [3], D-MDETR [9]) that learn end-to-end vision-language representations show promising performance in these more challenging scenarios. Our proposed M²IST further strengthens the vision-language representation learning by combining the channel-level and token-level vision-language alignment, thus achieving impressive performance on the RefCOCOg benchmark.

In summary, Table II illustrates that M²IST achieves an optimal performance-efficiency trade-off compared to listed full fine-tuning methods, underscoring its advantage in **parameter efficiency**, as discussed in Section III-C.

c) Comparison of Time Efficiency: We present the training and inference speeds on RefCOCO dataset of full fine-tuning, standard adapter-tuning [12], and our M²IST in Table III.

TABLE IV

COMPARISON ON REFERITGAME. BOTH THE STANDARD ADAPTER AND OUR M²IST USE THE SAME BASE ARCHITECTURE.

Methods	Parameters↓ (M)	Memory ↓ (GB)	ReferItGame val	test
Adapter	3.27 (2.17%)	28.52 (73.22%)	57.28	56.89
M ² IST	3.19 (2.11%)	15.44 (39.64%)	60.61	59.30

For training speed, it is evident that PETL methods improve training speed compared to full fine-tuning. This improvement is largely due to the reduced number of parameters that need to be updated when using PETL methods. Notably, M²IST achieves greater efficiency than adapter-tuning in terms of training time by updating parameters in parallel with pre-trained encoders, achieving approximately 36.54% faster than full fine-tuning. For inference speed, while adapter-tuning slightly reduces inference speed, our M²IST maintains it. This is attributed to the fact that, during inference, M²IST operates in parallel with the pre-trained encoders, maintaining inference speed. In contrast, standard adapters are inserted within the pre-trained encoders, leading to lower computational efficiency. These findings are consistent with the advantage in **time efficiency** proposed in Section III-C.

In summary, M²IST is Pareto-optimal in terms of accuracy, parameter efficiency, memory efficiency, and time efficiency. By tuning only 3.19M encoder parameters (**2.11%** of fully fine-tuning) and requiring 15.44GB of GPU memory (**39.61%** of fully fine-tuning) and **63.46%** of the full fine-tuning time, M²IST makes fine-tuning a strong REC model on a single NVIDIA 3060 GPU (16GB).

d) Comparison on Phrase Grounding Task: To demonstrate the generalizability of our M²IST, we have conducted experiments with M²IST on the task of phrase grounding.

Phrase grounding is a challenging vision-language task that given a noun phrase, output the corresponding single or multiple object detection bounding boxes. If an entire sentence is input, then it's about localizing all the noun phrases included in the sentence. Here, we use the same base architecture in our paper for phrase grounding on ReferItGame dataset [57]. Table IV demonstrates the generalization ability of our M²IST in understanding multi-object scenarios, while also exhibiting significant parameter and memory efficiency during fine-tuning.

D. Ablation Study and Analysis

In this sub-section, we investigate the impact of various factors in M²IST. All experiments in this section are performed on three sets of RefCOCO [22] dataset.

a) Effects of Different Components of M³ISA: We present the efficiency and performance of various components of M³ISA to examine their effects, as shown in Table V.

We can see that: **(1)** Freezing the encoders and only training the V-L Encoder leads to much greater performance degradation (Table V (a)), indicating a significant domain gap between the pre-trained domains of the two encoders and the REC domain. **(2)** Fine-tuning single-modality adapters (LEA/VEA) significantly enhances performance compared to using frozen encoders (Table V (b,c)). Specifically, VEA provides greater

TABLE V

ABLATION ON DIFFERENT COMPONENTS IN M³ISA. WITHOUT ADDING ANY COMPONENT OF M³ISA, IT CAN BE VIEWED AS FREEZING THE PRE-TRAINED ENCODER AND ONLY TRAINING THE V-L ENCODER.

#	LEA	VEA	IEA	Params.↓ (M)	Mem.↓ (GB)	RefCOCO		
						val	testA	testB
(a)				0	14.32	72.72	73.33	71.27
(b)	✓			0.59	14.90	77.08	77.82	73.38
(c)		✓		1.02	14.52	78.30	78.95	73.58
(d)	✓	✓		1.61	15.09	79.39	79.18	74.41
(e)			✓	1.58	14.84	78.85	79.01	73.87
(f)	✓	✓	✓	3.19	15.44	81.35	82.29	77.98

TABLE VI

EFFECTS OF DIFFERENT MIXING STRATEGIES OF M³ISA. "VEA+LEA" AND "IEA+IEA" REFER TO ADOPTING THE INTRA-MODALITY ADAPTERS AND THE INTER-MODALITY ADAPTERS, RESPECTIVELY.

#	Multi-head Attention	Multi-layer Perceptron	Params.↓ (M)	Mem.↓ (GB)	RefCOCO		
					val	testA	testB
<i>Same adapters mixing</i>							
(a)	LEA+VEA	LEA+VEA	3.22	15.65	79.87	80.52	76.33
(b)	IEA+IEA	IEA+IEA	3.17	14.84	78.72	80.05	76.01
<i>Different adapters mixing</i>							
(c)	LEA+VEA	IEA+IEA	3.19	15.38	80.58	81.26	76.65
(d)	IEA+IEA	LEA+VEA	3.19	15.44	81.35	82.29	77.98

performance improvement compared to LEA, suggesting that adapting visual representation plays a more crucial role in object perception and localization than language representation. **(3)** Combining LEA and VEA yields similar performance to using IEA alone (Table V (d,e)). This indicates that using either can bring around 6% accuracy improvement compared to freezing the encoders. **(4)** Incorporating LEA, VEA, and IEA into M³ISA results in an average improvement of 8.10% across the three sets of RefCOCO, achieving the best performance among these ablation variants (Table V (f)). It is worth noting that fine-tuning each ablation variant of M³ISA incurs at most an additional **1.12GB** of GPU memory compared to freezing the encoder, demonstrating the **memory efficiency** of M²IST (see Section III-C).

b) Effects of Different Mixing Strategies of M³ISA:

In Table VI, to further investigate the effects of different adapter combination forms (i.e., mixing strategies), we present the performance of adopting intra-modality adapters or inter-modality adapters in parallel with different pre-trained layers (MHA and FFN). The findings are as follows: **(1)** Transferring pre-trained single-modality knowledge to the REC domain (e.g., LEA+VEA) is more effective in accurately locating the referred object than merely achieving cross-modality interaction (e.g., IEA+IEA) (Table VI (a,b)). **(2)** Combining intra-modality adapters and inter-modality adapters enhances performance, indicating that joint transfer of pre-trained single-modality knowledge and cross-modality interaction aids in accurately localizing referred objects by text descriptions (Table VI (a,b,c,d)). This observation aligns with findings from other challenging vision-language tasks [8], [16], suggesting that combining deep inter-modality fusion with intra-modality adaptation improves performance. **(3)** The best performance among the M³ISA variants is achieved by first connecting the vision and language encoders with IEAs, and then adapting

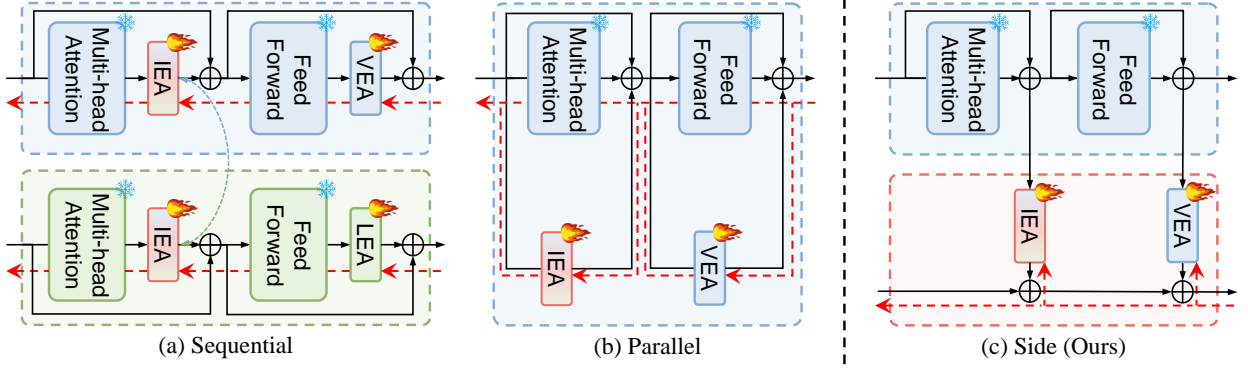


Fig. 3. **Different adapter insertion forms.** During fine-tuning, gradients in (a) and (b) backpropagate through the heavy encoders, while gradients in (c) only backpropagate through the lightweight adapters, achieving memory-efficient tuning for REC. Note that (b) and (c) only illustrate the vision branch for simplicity.

TABLE VII

EFFECTS OF DIFFERENT INSERTION FORMS OF M^3ISA . "SEQUENTIAL" AND "PARALLEL", AND "SIDE" CORRESPOND TO (A), (B), AND (C) IN FIGURE 3, RESPECTIVELY.

#	Insertion forms	Params.↓ (M)	Mem.↓ (GB)	RefCOCO		
				val	testA	testB
(a)	Sequential	3.19	27.19	78.76	80.25	74.90
(b)	Parallel	3.19	20.37	78.29	78.71	75.30
(c)	Side	3.19	15.44	81.35	82.29	77.98

TABLE VIII

EFFECTS OF DIFFERENT INSERTION POSITIONS OF M^3ISA . THE VISION ENCODER AND LANGUAGE ENCODER CONSIST OF 6 AND 12 TRANSFORMER ENCODER LAYERS, RESPECTIVELY. "1 → 6" DENOTES THE ADDITION OF M^3ISAs IN THE 1ST THROUGH 6TH ENCODER LAYERS.

#	Vision Encoder	Language Encoder	RefCOCO		
			val	testA	testB
(a)	1 → 6	1 → 6	80.65	81.86	77.39
(b)	1 → 6	[1,3,5,7,9,11]	80.83	81.76	77.54
(c)	1 → 6	7 → 12	81.35	82.29	77.98

the interacted features and single-modality features to the REC domain with VEA and LEA (Table VI (a,b,c,d)).

c) *Effects of Different Insertion Forms of M^3ISA :* As depicted in Figure 3 and Table VII, we evaluate the impact of integrating M^3ISAs with different insertion forms on performance and GPU memory usage. From Table VII, we can observe that: (1) Side insertion yields the best performance. We suppose that implementing M^3ISAs on *side networks* enhances the alignment between the referring sentence and the referred object, resulting in improved localization performance. (2) In terms of fine-tuning efficiency, all three insertion forms contribute to a reduction in GPU memory usage to varying degrees. It is evident that incorporating M^3ISAs into the *side networks* consumes the least amount of GPU memory. This is because the gradients backpropagate through the lightweight M^3ISAs instead of heavy encoders. This aligns with the **memory efficiency** advantage mentioned in Section III-C.

d) *Effects of Different Insertion Positions of M^3ISA :* As illustrated in Table VIII, we further investigate the impact of introducing M^3ISAs at different positions within the pre-trained Vision Encoder and Language Encoder. The Vision Encoder and Language Encoder consist of 6 and 12 transformer encoder layers, respectively, and the IEA needs to be inserted into the encoder layers at the same indices. We explore three common

TABLE IX

EFFECTS OF DIFFERENT INTERACTION DIMENSIONS OF M^3ISA . " C_i " REPRESENTS THE INTERACTION DIMENSION OF INTERACTION EXPERT ADAPTER (IEA) IN M^3ISAs .

#	C_i	Params.↓ (M)	Mem.↓ (GB)	RefCOCO		
				val	testA	testB
(a)	64	2.00	15.34	77.31	77.87	73.27
(b)	128	2.40	15.35	79.26	79.58	74.60
(c)	256	3.19	15.44	81.35	82.29	77.98

TABLE X

EFFECTS OF COMBINING M^2IST WITH LoRA. "FULL" REPRESENTS FULLY FINE-TUNING THE BASELINE MODAL.

Methods	Params.↓ (M)	Mem.↓ (GB)	RefCOCO		
			val	testA	testB
Full	151	38.95	80.32	82.67	75.24
LoRA	2.37	20.37	77.57	78.22	73.37
M^2IST	3.19	15.44	81.35	82.29	77.98
$M^2IST+LoRA$	6.46	21.68	81.83	82.83	77.54

insertion forms, as shown in Table VIII (a-c). It is evident that inserting M^3ISAs in parallel to the deeper encoder layers of the pre-trained Language Encoder results in better performance. We suggest that deeper encoder layers contain richer semantic features, and establishing cross-modality interaction on this basis helps the model learn finer region-text alignment, thereby achieving better localization performance.

e) *Effects of Different Interaction Dimensions of M^3ISA :* We further ablate the impact of changing the interaction dimensions C_i of inter-modality adapters (i.e., IEA), and follow the paradigm of Table VI (d). As depicted in Table IX, deeper cross-modality interaction provides better vision-language channel-level alignment, thus resulting in an increase in performance. Thus, C_i is set to 256 to achieve the optimal trade-off among accuracy, number of tunable parameters, and GPU memory consumption. It is worth noting that all ablative variants exhibit a remarkable level of memory efficiency, as they consume less than 16GB of GPU memory. This observation is consistent with the **memory efficiency** advantage highlighted in Section III-C.

f) *Effects of Combining M^2IST with LoRA:* To evaluate the extensibility of our M^2IST , we combine it with the widely used PETL method, LoRA [13].

As shown in Table X, using LoRA alone leads to performance degradation. This is because LoRA integrates two pairs of tunable low-rank decomposed weight matrices into

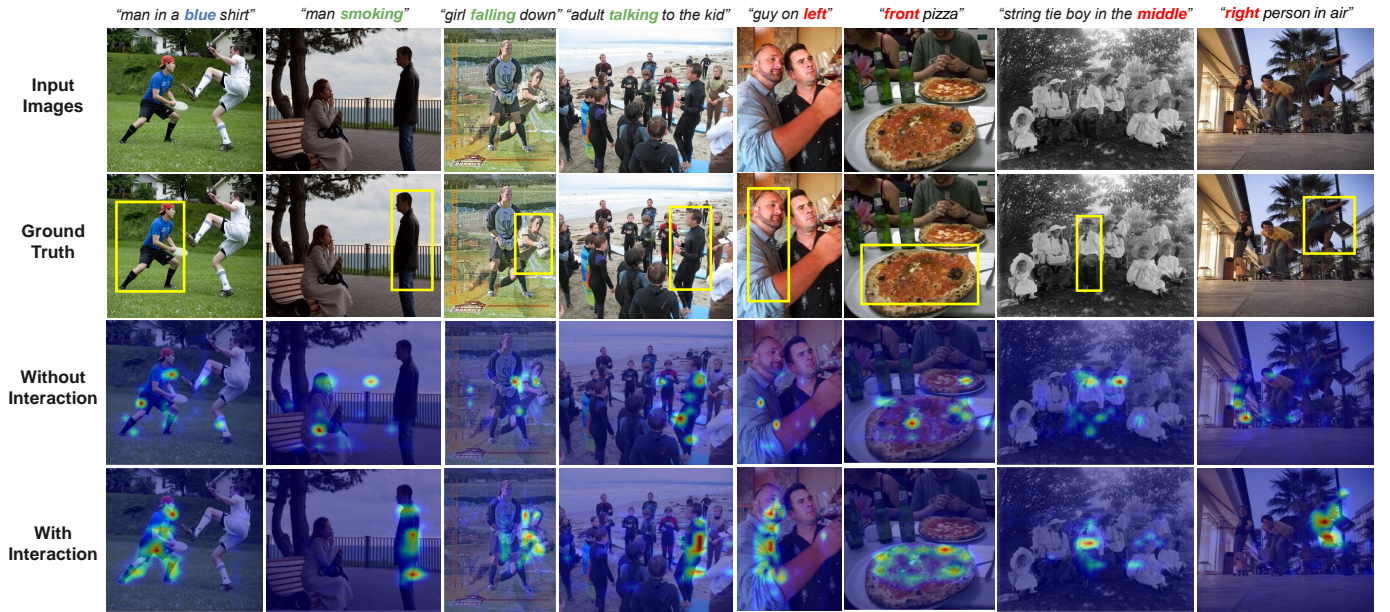


Fig. 4. Visualizations of attention maps from the V-L Encoder with different mixing strategies. Cases include object appearance attributes (blue words), human actions (green words), and spatial relations (red words).

each encoder layer of the Vision Encoder and Language Encoder separately, without any multi-modality interaction during the feature extraction stage. Combining M²IST with LoRA performs comparably to or even better than using M²IST alone, demonstrating the extensibility of our approach. However, as discussed in Section III-C, such a combination may significantly increase the number of updated parameters and GPU memory usage, thus undermining the memory efficiency advantage of M²IST. Therefore, our M²IST achieves the optimal performance and efficiency trade-off in this comparison.

E. Qualitative Results

To investigate the impact of cross-modality interaction facilitated by M³ISA, we visualize the attention maps from the V-L Encoder. We compare M³ISA (referred to as "With Interaction") with its variant presented in Table VI (referred to as "Without Interaction") across various scenarios to assess their effectiveness in understanding challenging cases, such as human action recognition and spatial relation reasoning, as shown in Figure 4.

It is clear that M³ISA effectively addresses diverse REC cases, particularly in spatial relations. For instance, in the sixth case, the "With Interaction" approach successfully directs attention to the front region associated with the referring sentence "front pizza". This is especially evident in the last case, where "With Interaction" focuses more on the area corresponding to the referring sentence "right person in air", while "Without Interaction" fails to identify the correct region. These visualization results demonstrate that the enhanced cross-modality interaction facilitated by the IEA enables effective comprehension of complex semantic information.

V. CONCLUSION

In this paper, we introduce Multi-Modal Interactive Side-Tuning (M²IST), an efficient tuning method designed for

referring expression comprehension. Based on this framework, we introduce Mixture of Multi-Modal Interactive Side Adapters (M³ISA) to efficiently transfer pre-trained single-modality knowledge and facilitate cross-modality interaction between vision and language encoders. During fine-tuning, we freeze the pre-trained vision-language foundation models and update M³ISAs on side networks, achieving efficient tuning for REC. By updating only 3.14M encoder parameters (2.11% of full fine-tuning) and using 15.44GB of GPU memory (39.61% of full fine-tuning), M²IST achieves competitive performance compared to full fine-tuning methods and outperforms other PETL methods across three benchmarks.

REFERENCES

- [1] L. Yu, Z. Lin, X. Shen *et al.*, "MAttNet: Modular attention network for referring expression comprehension," in *IEEE Conf. Comput. Vis. Pattern Recog.*, 2018, pp. 1307–1315.
- [2] Z. Yang, B. Gong, L. Wang, W. Huang, D. Yu, and J. Luo, "A fast and accurate one-stage approach to visual grounding," in *Int. Conf. Comput. Vis.*, 2019, pp. 4683–4693.
- [3] J. Deng, Z. Yang, T. Chen, W. Zhou, and H. Li, "Transvg: End-to-end visual grounding with transformers," in *Int. Conf. Comput. Vis.*, 2021, pp. 1769–1779.
- [4] G. Hua, M. Liao, S. Tian, Y. Zhang, and W. Zou, "Multiple relational learning network for joint referring expression comprehension and segmentation," *IEEE Trans. Multimedia*, vol. 25, pp. 8805–8816, 2023.
- [5] H. Qiu, L. Wang, T. Zhao, F. Meng, Q. Wu, and H. Li, "Mcce-rec: Mllm-driven cross-modal contrastive entropy model for zero-shot referring expression comprehension," *IEEE Trans. Circuit Syst. Video Technol.*, 2024.
- [6] Z. Ji, J. Wu, Y. Wang, A. Yang, and J. Han, "Progressive semantic reconstruction network for weakly supervised referring expression grounding," *IEEE Trans. Circuit Syst. Video Technol.*, 2024.
- [7] M. Sun, W. Suo, P. Wang, Y. Zhang, and Q. Wu, "A proposal-free one-stage framework for referring expression comprehension and generation via dense cross-attention," *IEEE Trans. Multimedia*, vol. 25, pp. 2446–2458, 2022.
- [8] C. Shang, H. Li, H. Qiu, Q. Wu, F. Meng, T. Zhao, and K. N. Ngan, "Cross-modal recurrent semantic comprehension for referring image segmentation," *IEEE Trans. Circuit Syst. Video Technol.*, vol. 33, no. 7, pp. 3229–3242, 2022.

- [9] F. Shi, R. Gao, W. Huang, and L. Wang, "Dynamic mdetr: A dynamic multimodal transformer decoder for visual grounding," *IEEE Trans. Pattern Anal. Mach. Intell.*, vol. 46, no. 2, pp. 1181–1198, 2024.
- [10] S. Huang, B. Gong, Y. Pan, J. Jiang, Y. Lv, Y. Li, and D. Wang, "VoP: Text-video co-operative prompt tuning for cross-modal retrieval," in *IEEE Conf. Comput. Vis. Pattern Recog.*, 2023, pp. 6565–6574.
- [11] Y. Yuan, Y. Zhan, and Z. Xiong, "Parameter-efficient transfer learning for remote sensing image-text retrieval," *IEEE Trans. Geosci. Remote Sens.*, 2023.
- [12] N. Houlsby, A. Giurgiu, S. Jastrzebski, B. Morrone, Q. De Laroussilhe, A. Gesmundo, M. Attariyan, and S. Gelly, "Parameter-efficient transfer learning for nlp," in *Int. Conf. Mach. Learn.*, 2019, pp. 2790–2799.
- [13] E. J. Hu, P. Wallis, Z. Allen-Zhu, Y. Li, S. Wang, L. Wang, W. Chen *et al.*, "LoRA: Low-rank adaptation of large language models," in *Int. Conf. Learn. Represent.*, 2022.
- [14] M. Jia, L. Tang, B.-C. Chen, C. Cardie, S. Belongie, B. Hariharan, and S.-N. Lim, "Visual prompt tuning," in *Eur. Conf. Comput. Vis.*, 2022, pp. 709–727.
- [15] S. Chen, C. Ge, Z. Tong, J. Wang, Y. Song, J. Wang, and P. Luo, "Adapt-former: Adapting vision transformers for scalable visual recognition," in *Adv. Neural Inform. Process. Syst.*, vol. 35, 2022, pp. 16 664–16 678.
- [16] Z. Xu, Z. Chen, Y. Zhang, Y. Song, X. Wan, and G. Li, "Bridging vision and language encoders: Parameter-efficient tuning for referring image segmentation," in *Int. Conf. Comput. Vis.*, 2023, pp. 17 503–17 512.
- [17] S. Huang, B. Gong, Y. Feng, M. Zhang, Y. Lv, and D. Wang, "Troika: Multi-path cross-modal traction for compositional zero-shot learning," in *IEEE Conf. Comput. Vis. Pattern Recog.*, 2024, pp. 24 005–24 014.
- [18] W. Wu, R. Tsao, Y. He, Y. Peng, L. Qin, and Q. Yin, "Visual grounding with dual knowledge distillation," *IEEE Trans. Circuit Syst. Video Technol.*, 2024.
- [19] M. Lu, R. Li, F. Feng, Z. Ma, and X. Wang, "Lgr-net: Language guided reasoning network for referring expression comprehension," *IEEE Trans. Circuit Syst. Video Technol.*, 2024.
- [20] N. Carion, F. Massa, G. Synnaeve, N. Usunier, A. Kirillov, and S. Zagoruyko, "End-to-end object detection with transformers," in *Eur. Conf. Comput. Vis.*, 2020, pp. 213–229.
- [21] J. Devlin, M.-W. Chang, K. Lee, and K. Toutanova, "Bert: Pre-training of deep bidirectional transformers for language understanding," *arXiv preprint arXiv:1810.04805*, 2018.
- [22] L. Yu, P. Poirson, S. Yang, A. C. Berg, and T. L. Berg, "Modeling context in referring expressions," in *Eur. Conf. Comput. Vis.*, 2016, pp. 69–85.
- [23] J. Mao, J. Huang, A. Toshev, O. Camburu, A. L. Yuille, and K. Murphy, "Generation and comprehension of unambiguous object descriptions," in *IEEE Conf. Comput. Vis. Pattern Recog.*, 2016, pp. 11–20.
- [24] V. K. Nagaraja, V. I. Morariu, and L. S. Davis, "Modeling context between objects for referring expression understanding," in *Eur. Conf. Comput. Vis.*, 2016, pp. 792–807.
- [25] L. Yang, Y. Xu, C. Yuan, W. Liu, B. Li, and W. Hu, "Improving visual grounding with visual-linguistic verification and iterative reasoning," in *IEEE Conf. Comput. Vis. Pattern Recog.*, 2022, pp. 9499–9508.
- [26] C. Zhu, Y. Zhou, Y. Shen, G. Luo, X. Pan, M. Lin, C. Chen, L. Cao, X. Sun, and R. Ji, "SeqTR: A simple yet universal network for visual grounding," in *Eur. Conf. Comput. Vis.*, 2022, pp. 598–615.
- [27] D. Liu, H. Zhang, F. Wu *et al.*, "Learning to assemble neural module tree networks for visual grounding," in *Int. Conf. Comput. Vis.*, 2019, pp. 4673–4682.
- [28] Y. W. Chen, Y. H. Tsai, T. Wang, Y. Y. Lin, and M. H. Yang, "Referring expression object segmentation with caption-aware consistency," in *Brit. Mach. Vis. Conf.*, 2019.
- [29] S. Ren, K. He, R. Girshick, and J. Sun, "Faster r-cnn: Towards real-time object detection with region proposal networks," *IEEE Trans. Pattern Anal. Mach. Intell.*, vol. 39, no. 6, pp. 1137–1149, 2016.
- [30] R. Hong, D. Liu, X. Mo, X. He, and H. Zhang, "Learning to compose and reason with language tree structures for visual grounding," *IEEE Trans. Pattern Anal. Mach. Intell.*, vol. 44, no. 2, pp. 684–696, 2019.
- [31] Y. Liao, S. Liu, G. Li, F. Wang, Y. Chen, C. Qian, and B. Li, "A real-time cross-modality correlation filtering method for referring expression comprehension," in *IEEE Conf. Comput. Vis. Pattern Recog.*, 2020, pp. 10 880–10 889.
- [32] Z. Yang, T. Chen, L. Wang, and J. Luo, "Improving one-stage visual grounding by recursive sub-query construction," in *Eur. Conf. Comput. Vis.*, 2020, pp. 387–404.
- [33] J. Ye, X. Lin, L. He, D. Li, and Q. Chen, "One-stage visual grounding via semantic-aware feature filter," in *ACM Int. Conf. Multimedia*, 2021, pp. 1702–1711.
- [34] J. Redmon and A. Farhadi, "Yolov3: An incremental improvement," *arXiv preprint arXiv:1804.02767*, 2018.
- [35] Y. Du, Z. Fu, Q. Liu, and Y. Wang, "Visual grounding with transformers," in *Int. Conf. Multimedia and Expo*, 2022, pp. 1–6.
- [36] T. Liu, X. Liu, L. Shi, Z. Xu, S. Huang, Y. Xin, and Q. Yin, "Sparse-Tuning: Adapting vision transformers with efficient fine-tuning and inference," *arXiv preprint arXiv:2405.14700*, 2024.
- [37] L. Yan, C. Han, Z. Xu, D. Liu, and Q. Wang, "Prompt learns prompt: exploring knowledge-aware generative prompt collaboration for video captioning," in *IJCAI*, 2023, pp. 1622–1630.
- [38] S. Bai, M. Zhang, W. Zhou, S. Huang, Z. Luan, D. Wang, and B. Chen, "Prompt-based distribution alignment for unsupervised domain adaptation," in *AAAI Conf. Artif. Intell.*, vol. 38, no. 2, 2024, pp. 729–737.
- [39] S. Jie and Z.-H. Deng, "Fact: Factor-tuning for lightweight adaptation on vision transformer," in *AAAI Conf. Artif. Intell.*, vol. 37, no. 1, 2023, pp. 1060–1068.
- [40] H. Jiang, J. Zhang, R. Huang, C. Ge, Z. Ni, J. Lu, J. Zhou, S. Song, and G. Huang, "Cross-modal adapter for text-video retrieval," *arXiv preprint arXiv:2211.09623*, 2022.
- [41] M. Cao, H. Tang, J. Huang, P. Jin, C. Zhang, R. Liu, L. Chen, X. Liang, L. Yuan, and G. Li, "Rap: Efficient text-video retrieval with sparse-and-correlated adapter," in *Findings of the Association for Computational Linguistics: ACL 2024*, 2024.
- [42] J. O. Zhang, A. Sax, A. Zamir, L. Guibas, and J. Malik, "Side-tuning: a baseline for network adaptation via additive side networks," in *Eur. Conf. Comput. Vis.*, 2020, pp. 698–714.
- [43] Y.-L. Sung, J. Cho, and M. Bansal, "LST: Ladder side-tuning for parameter and memory efficient transfer learning," in *Adv. Neural Inform. Process. Syst.*, vol. 35, 2022, pp. 12 991–13 005.
- [44] M. Fu, K. Zhu, and J. Wu, "DTL: Disentangled transfer learning for visual recognition," in *AAAI Conf. Artif. Intell.*, vol. 38, no. 11, 2024, pp. 12 082–12 090.
- [45] K. He, X. Zhang, S. Ren, and J. Sun, "Deep residual learning for image recognition," in *IEEE Conf. Comput. Vis. Pattern Recog.*, 2016, pp. 770–778.
- [46] A. Vaswani, N. Shazeer, N. Parmar, J. Uszkoreit, L. Jones, A. N. Gomez, L. Kaiser, and I. Polosukhin, "Attention is all you need," in *Adv. Neural Inform. Process. Syst.*, vol. 30, 2017, pp. 5998–6008.
- [47] Z. Huang and S. Satoh, "Referring image segmentation via joint mask contextual embedding learning and progressive alignment network," in *Proceedings of the Conference on Empirical Methods in Natural Language Processing*, 2023, pp. 7753–7762.
- [48] X. Liu, S. Huang, Y. Kang, H. Chen, and D. Wang, "VGDiffZero: Text-to-image diffusion models can be zero-shot visual grounders," in *IEEE Int. Conf. Acoust. Speech Signal Process.*, 2024, pp. 2765–2769.
- [49] T.-Y. Lin, M. Maire, S. Belongie, J. Hays, P. Perona, D. Ramanan, P. Dollár, and C. L. Zitnick, "Microsoft coco: Common objects in context," in *Eur. Conf. Comput. Vis.*, 2014, pp. 740–755.
- [50] Y. Zhu, R. Kiros, R. Zemel, R. Salakhutdinov, R. Urtasun, A. Torralba, and S. Fidler, "Aligning books and movies: Towards story-like visual explanations by watching movies and reading books," in *Int. Conf. Comput. Vis.*, 2015.
- [51] H. Zhang, Y. Niu, and S.-F. Chang, "Grounding referring expressions in images by variational context," in *IEEE Conf. Comput. Vis. Pattern Recog.*, 2018, pp. 4158–4166.
- [52] B. Zhuang, Q. Wu, C. Shen, I. Reid, and A. Van Den Hengel, "Parallel attention: A unified framework for visual object discovery through dialogs and queries," in *IEEE Conf. Comput. Vis. Pattern Recog.*, 2018, pp. 4252–4261.
- [53] Y. Liao, S. Liu, G. Li, F. Wang, Y. Chen, C. Qian, and B. Li, "A real-time cross-modality correlation filtering method for referring expression comprehension," in *IEEE Conf. Comput. Vis. Pattern Recog.*, 2020, pp. 10 880–10 889.
- [54] Y. Zhou, R. Ji, G. Luo, X. Sun, J. Su, X. Ding, C.-W. Lin, and Q. Tian, "A real-time global inference network for one-stage referring expression comprehension," *IEEE Trans. Neural Networks Learn. Syst.*, vol. 34, no. 1, pp. 134–143, 2021.
- [55] Y. Zhou, T. Ren, C. Zhu, X. Sun, J. Liu, X. Ding, M. Xu, and R. Ji, "Trar: Routing the attention spans in transformer for visual question answering," in *Int. Conf. Comput. Vis.*, 2021, pp. 2074–2084.
- [56] Z. Zhang, Z. Wei, Z. Huang, R. Niu, and P. Wang, "One for all: One-stage referring expression comprehension with dynamic reasoning," *Neurocomputing*, vol. 518, pp. 523–532, 2023.
- [57] S. Kazemzadeh, V. Ordonez, M. Matten, and T. Berg, "ReferItGame: Referring to objects in photographs of natural scenes," in *Proceedings of the Conference on Empirical Methods in Natural Language Processing*, 2014.